The Haldane phase at finite temperatures: a defect approach

1992 J. Phys.: Condens. Matter 4 7899

(http://iopscience.iop.org/0953-8984/4/39/005)

J. Phys.: Condens. Matter 4 (1992) 7899–7912. Printed in the UK

The Haldane phase at finite temperatures: a defect approach

Holger Köhler and Rolf Schilling

Institut für Physik, Johannes Gutenberg-Universität Mainz, Staudingerweg 7, D-6500 Mainz, Federal Republic of Germany

Received 11 May 1992, in final form 1 July 1992

Abstract. Here we investigate a one-dimensional, spin $s = 1$ Heisenberg antiferromagnet with exchange and single-ion anisotropy. A self-consistent approach using defects, which was recently proposed by Gómez-Santos, is applied to determine the phase diagram at $T = 0$ K and is generalized to finite temperatures. The phase diagram for exchange anisotropy constant $\epsilon \geqslant 1$ is in reasonable agreement with earlier numerical results; the three different phases (Néel, Haldane and large-D phases) can be characterized by the defect concentration.

It is shown that the ground state and the excitations are BCS-like. The Haldane phase can be interpreted as a BCS phase in particular, and the lowest excitations, as a break-up of 'Cooper pairs'. The specific heat C exhibits a maximum. Its position T_{max} increases with increasing gap energy E_g; below T_{max}, there exists a regime with linear temperature dependence.

1. Introduction

In 1983 Haldane [1] predicted that integral-spin antiferromagnetic Heisenberg spin chains have a finite gap $E_g > 0$, in contrast to half-integral spin chains, which are gapless. Haldane arrived at this result by mapping the Heisenberg antiferromagnet onto a nonlinear σ model. Subsequently, the conjecture has been confirmed for different spin Hamiltonians, and rigorous proof was given for an isotropic Heisenberg model including a special type of biquadratic exchange [2]. A review summarizing the different models and approaches, also including experimental confirmation [3], was recently given by Affleck [4].

In this paper we will consider a spin $s = 1$ Heisenberg chain with antiferromagnetic, anisotropic exchange interaction and crystal field anisotropy. The Hamiltonian is given as

$$H = \sum_n [S_n^x S_{n+1}^x + S_n^y S_{n+1}^y + \epsilon S_n^z S_{n+1}^z] + D \sum_n (S_n^z)^2 . \tag{1}$$

Botet *et al* [4] were the first to do a numerical investigation of this Hamiltonian in order to prove that the Haldane phase exists in a finite region of the $(\epsilon - D)$ parameter space. Meanwhile, a unique phase diagram has emerged for the Hamiltonian ((1)) [5,6,7]. For $\epsilon \geqslant 0$, three different phases exist, i. e. the Néel phase, the Haldane phase and the large-D phase, which can be distinguished by different types of order parameters [6]; moreover, the gap energy E_g vanishes on the boundaries between the Haldane phase and the other two phases. While most of these results are based on

0953-8984/92/397899+14$04.50

numerical calculations for finite chains [5,6], an analytical approach by Tasaki [7] has yielded exact bounds for the phase boundaries — although within a restricted Hilbert space.

Gómez-Santos recently proposed an attractive approach to model (equation (1)), with $D = 0$ and spin quantum number $s = 1$ [8]. Starting from the Néel state, local defects with fermionic character were introduced, and the original spin Hamiltonian was transformed to a fermion system with two-fermion interactions, whereby restricting the original Hilbert space to a subspace H_0. Owing to the interactions, the fermion Hamiltonian cannot be treated exactly, but a Hartree–Fock approximation finally led to the result in which there is a gap which just vanishes at $\epsilon_c \approx 1.125$ (for $D = 0$) [9]. An extension of subspace H_0 led to an improved value $\epsilon_c \approx 1.184$, which compares very favorably with quantum Monte Carlo calculations (e. g. [5]). An outline of the defect method is given in the next section.

There is not much work available on the temperature dependence of the Haldane phase and the phase diagram of Hamiltonian ((1)) in general. Recently, however, Delica *et al* [10] calculated the T-dependence of the susceptibility for $\epsilon = 1$ and $D \geqslant 0$ within the Haldane phase, and these results are consistent with the existence of an energy gap.

Numerical calculations [11] and *experimental* results [12] for the magnetic part of the specific heat are available for spin $s = 1$ quantum chains; and in both cases a Schottky anomaly was found. The results attained by Moses *et al* [12] are also compatible with a linear T-dependence within a finite temperature range below T_{max}, the location of the Schottky anomaly.

The purpose of this paper is twofold:

(i) to investigate to what extent the description by defects is reasonable for $D \neq 0$, and in particular to check whether the phase diagram in $(\epsilon - D)$ space can be reproduced;

(ii) to extend the defect method to finite temperatures, in order to study the temperature dependence of the phase diagram, the gap energy, and the specific heat.

Our paper is organized as follows: section 2 gives an outline of the defect method and its application to Hamiltonian ((1)). In section 3 we present our results; finally, section 4 contains a discussion of these results and some conclusions.

2. Defect approach

Here we describe the defect pattern suggested by Gómez-Santos [8], considering only $s = 1$. The perfect antiferromagnetic order of the Néel state in one dimension

$$\ldots \uparrow\downarrow\uparrow\downarrow\uparrow\downarrow\uparrow\downarrow \ldots$$

is destroyed due to 'spin-zero defects' (SZD)

$$\ldots \uparrow\downarrow\uparrow\downarrow \bigcirc \uparrow\downarrow\uparrow \ldots ,$$

(a spin-zero defect is a localized defect at a site i is in the state with $S_n^z = 0$). Next, a restriction of the 3^N-dimensional Hilbert space H_0 is introduced. Only the following local spin configurations are considered:

$$|\ldots \uparrow\downarrow\uparrow\downarrow\uparrow\downarrow \ldots\rangle \qquad |\ldots \uparrow\downarrow \bigcirc \uparrow\downarrow\uparrow \ldots\rangle$$
$$\lambda_1|\ldots \uparrow\downarrow \bigcirc\bigcirc \uparrow\downarrow \ldots\rangle - \lambda_2|\ldots \uparrow\downarrow\uparrow\uparrow\downarrow \ldots\rangle \qquad (2)$$

with $\lambda_1^2 + \lambda_2^2 = 1$ (λ_1 and λ_2 are real). The latter superposition accounts for ferromagnetic correlations, provided $\lambda_1 \neq 1$. Note that the nonzero spins adjacent to the SZD are always in antiferromagnetic order. It is aimed to describe the defects as fermions. Now, in order to derive an effective fermion Hamiltonian, the action of the various parts of (1) on the restricted set (2) of spin configurations is studied:

(i) $x - y$ part

The $x - y$ part can be rewritten as

$$\tfrac{1}{2}(S_i^+ S_{i+1}^- + S_i^- S_{i+1}^+) \tag{3}$$

Its effects are threefold:

First, an SZD is shifted by one lattice constant, e.g.

$$\ldots \uparrow\downarrow \bigcirc \uparrow\downarrow\uparrow \leftrightarrow \uparrow\downarrow\uparrow \bigcirc \downarrow\uparrow \ldots .$$

This hopping can be described by

$$[1 + (\lambda_1 - 1)(n_{i-1} + n_{i+2})] c_i^\dagger c_{i+1} + \text{HC} \tag{4}$$

where $n_i = c_i^\dagger c_i$ is the occupation operator at ith site; and c_i and $c_i^\dagger$ are fermion annihilation and creation operators. The second term in (4) considers two SZD which are next-nearest neighbours.

Second, transitions are induced between the first and third state of (2):

$$\ldots \uparrow\downarrow \bigcirc\bigcirc \uparrow\downarrow \ldots \leftrightarrow \ldots \uparrow\downarrow\uparrow\downarrow\uparrow\downarrow \ldots$$

which can be represented as

$$\lambda_1 (c_i^\dagger c_{i+1}^\dagger + \text{HC}). \tag{5}$$

Third, transitions arise between both states of the superposition (third state of (2)):

$$\ldots \uparrow\downarrow \bigcirc\bigcirc \uparrow\downarrow \leftrightarrow \uparrow\downarrow\downarrow\uparrow\uparrow\downarrow \ldots$$

which yields an effective contribution

$$-2\lambda_1\lambda_2 n_i n_{i+1}. \tag{6}$$

(ii) $z - z$ part

This part consists of at most the Ising part and the single-ion anisotropy, and it is reproduced by

$$(2\epsilon - D)(n_i - 1) - (\epsilon\lambda_1^2 - 2D^2\lambda_2)\, n_{i+1} n_i + \epsilon \ . \tag{7}$$

Summing up equations (4)–(7), we obtain the effective fermion Hamiltonian

$$H_{\text{eff}} = \sum_i [c_i^\dagger c_{i+1} + \lambda_1 c_i^\dagger c_{i+1}^\dagger + \text{HC}] + \sum_i [(2\epsilon - D)\, n_i - \epsilon' n_i n_{i+1}]$$
$$+ (\lambda_1 - 1) \sum_i [(n_{i-1} + n_{i+2})\, c_i^\dagger c_{i+1} + \text{HC}] + \text{constant} \tag{8}$$

where

$$\epsilon' = 2\lambda_1\lambda_2 + \epsilon\lambda_1^2 - 2D\lambda_2^2. \tag{9}$$

A comparison with the corresponding Hamiltonian obtained by Gómez-Santos shows that the single-ion anisotropy renormalizes both the coupling constant ϵ' and the chemical potential of the defects. Unfortunately, the partition function cannot be calculated exactly. Following [8], a Hartree–Fock approximation(at finite temperature)

$$n_i n_{i+1} \to 2n_0 n_i - n_1\left(c_i^\dagger c_{i+1} + \text{HC}\right) + h_1\left(c_i^\dagger c_{i+1}^\dagger + \text{HC}\right) + \text{constant} \tag{10}$$

is performed. All other terms including four fermi operators are handled similarly. The *canonical* averages:

$$n_j = \langle c_i^\dagger c_{i+j}\rangle \qquad h_j = \langle c_i^\dagger c_{i+j}^\dagger\rangle \tag{11}$$

are determined in a self-consistent manner by using the Hartree–Fock Hamiltonian H_{HF}. After a Fourier transformation, H_{HF} takes the form

$$H_{\text{HF}} = \sum_q (c_q^\dagger c_{-q})\,(A_q\hat{\sigma}_z + B_q\hat{\sigma}_y)\begin{pmatrix} c_q \\ c_{-q}^\dagger \end{pmatrix} + \text{constant} \tag{12}$$

where $\hat{\sigma}_\alpha$ $(\alpha = x, y, z)$ are the Pauli matrices, and

$$c_q = \frac{1}{\sqrt{N}}\sum_n c_n e^{iqn} \tag{13}$$

$$\begin{aligned} A_q &= \epsilon_s + \nu\cos(q) + \omega\cos(2q) \\ B_q &= \nu'\sin(q) + \omega'\sin(2q) \\ \nu &= 1 + \epsilon n_1 + 2(\lambda_1 - 1)(n_0 - n_2) \\ \nu' &= \lambda_1 - \epsilon h_1 + 2(\lambda_1 - 1)h_2 \\ \omega &= -2n_1(\lambda_1 - 1) \qquad \omega' = 2h_1(\lambda_1 - 1) \\ \epsilon_s &= \epsilon - \tfrac{1}{2}D - n_0\epsilon' + 2n_1(\lambda_1 - 1). \end{aligned} \tag{14}$$

The Hamiltonian ((12)) is bilinear, and it can always be diagonalized [13]. This can be achieved by a Bogoljubov transformation

$$c_q = u_q^* d_q + v_q d_{-q}^\dagger \qquad c_q^\dagger = v_q^* d_{-q} + u_q d_q^\dagger \tag{15}$$

where

$$u_q = -\frac{1}{\sqrt{2}}(1 - \text{i})\cos\left(\frac{\Theta_q}{2}\right) v_q = -\frac{1}{\sqrt{2}}(1 + \text{i})\sin\left(\frac{\Theta_q}{2}\right). \tag{16}$$

It is easy to verify that the new operators d_q and $d_q^\dagger$ satisfy the fermion commutation relations. Angle Θ_q is determined such that the nondiagonal terms in the Hamiltonian (12) vanish, which yields

$$\tan\Theta_q = \frac{B_q}{A_q}. \tag{17}$$

With this transformation, it follows that

$$H_{\mathrm{HF}} = \sum_q E_q d_q^\dagger d_q + U \tag{18}$$

where the ground-state energy is

$$U = N[D + \epsilon_s - \epsilon + \epsilon' (n_0^2 - n_1^2 + h_1^2) - 4(n_0 n_1 - n_1 n_2 + h_1 h_2)(\lambda_1 - 1)] - \tfrac{1}{2}\sum_q E_q \tag{19}$$

and the one-particle excitation energies are

$$E_q = 2[(\epsilon_s + \nu \cos(q) + \omega \cos(2q))^2 + (\nu' \sin(q) + \omega' \sin(2q))^2]^{1/2}. \tag{20}$$

E_q is positive, and our numerical calculations show that the minimum excitation energy is taken either at the Brillouin center $q = 0$ or at its edge $q = \pi$. Using these results, the *self-consistency equations* for n_j and h_j become within the thermodynamic limit:

$$\begin{aligned} n_j &= \tfrac{1}{2}\delta_{0j} - \frac{1}{\pi}\int_0^\pi \mathrm{d}q \, \frac{A_q}{E_q} \tanh\left(\frac{\beta E_q}{2}\right) \cos(jq) \qquad j = 0,1,2 \\ h_j &= -\frac{1}{\pi}\int_0^\pi \mathrm{d}q \, \frac{B_q}{E_q} \tanh\left(\frac{\beta E_q}{2}\right) \sin(jq) \qquad j = 1,2 \\ \beta &= (kT)^{-1} \end{aligned} \tag{21}$$

where A_q, B_q and E_q depend on $\{n_j\}$, $\{h_j\}$ and λ_1 (cf equation (14)). The reader should note that the number of fermions is not conserved, but that it varies with the temperature and the chemical potential of the defects. The five self-consistency equations (21) are solved numerically for fixed λ_1, and λ_1 is obtained by minimizing the free energy.

3. Results

The self-consistency conditions (21) were solved numerically. One fixed point has been found only—that is to say, there is no phase transition with respect to the temperature, which is consistent with the one–dimensionality of our model. In the following, we will present the various physical quantities we have calculated from the solution of (21).

3.1. Ground state energy

Although the ground state energy U by itself is not of importance, its approximate value compared to direct numerical evaluation may already assess the quality of the approximations involved in our approach.

Unfortunately, we have not found values for U except for $U = -1.401$ [14] at the isotropic point $\epsilon = 1$, $D = 0$, which is within 0.1% of the result obtained with the defect method (see also [8]).

3.2. Phase diagram

More important is the phase diagram, which we explored for $\epsilon \geqslant 0$ only. Negative values for ϵ result in an instability of the numerical iteration of the self-consistency equations, which may be a hint that the defect method fails for $\epsilon \leqslant 0$. For $0 \leqslant \epsilon \leqslant 1$ and $D < 0$, we obtained an additional phase boundary not found in earlier work [4–7]. In this range, λ_1 differs significantly from unity, i.e. the ferromagnetic correlations are more important. These correlations were probably not taken into account well enough by the variational parameter λ_1. We therefore believe that the additional phase boundary that we found is an artifact. Consequently, only the results for $\epsilon \geqslant 1$ will be presented.

Since the gap energy E_g is the crucial quantity with respect to Haldane's conjecture, it is shown in figure 1 for $T = 0$. A channel for large ϵ and D exists, which bifurcates into a pair of channels for smaller ϵ and D. Within these channels, E_g is singular. Locating these singularities, we obtain the phase diagram which is depicted in figure 2. In agreement with the currently available results, we find three phases: the Néel, Haldane and large-D phases. At the phase boundaries between the Haldane phase and the other phases, E_g vanishes continuously, but with a discontinuity in its derivatives. Between the Néel phase and the large-D phase, E_g does not vanish, and it changes continuously. Our phase diagram (at $T = 0K$) is also consistent with the rigorous bounds derived by Tasaki [7] for a restricted Hilbert space; Tasaki has found that there is a Néel phase for $D < \epsilon - 2$ and a unique disordered ground state with exponential decay of the correlations (the Haldane and large-D phases) for $D > \frac{3}{2}\epsilon - 1$. A comparison of the phase diagram for $T = 0$ and $T = 2$ (see figure 2) demonstrates that the quality of the phase diagram does not change at finite temperatures. With increasing temperature, the triple point is shifted to $\epsilon = D = \infty$.

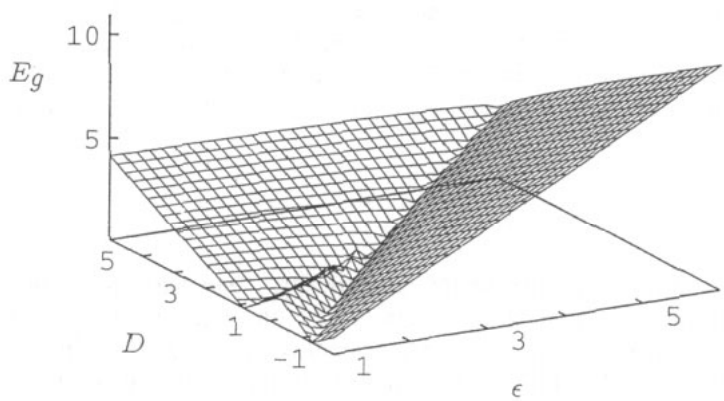

Figure 1. The gap energy E_g at $T = 0$ as a function of ϵ and D.

The following two figures, 3 and 4, show the T-dependence of the energy gap and of the defect concentration in the Haldane phase at the isotropic point, respectively. Qualitatively, the minimum in $E_g(T)$ is in agreement with the experiment [16]. Moving the parameter D closer to the phase boundary between the Haldane and the large-D phase gives rise to a maximum in E_g and n_0, in contrast to the isotropic point. In the Néel and large-D phase, n_0 increases and decreases monotonously. In both of these phases the energy gap decreases monotonously.

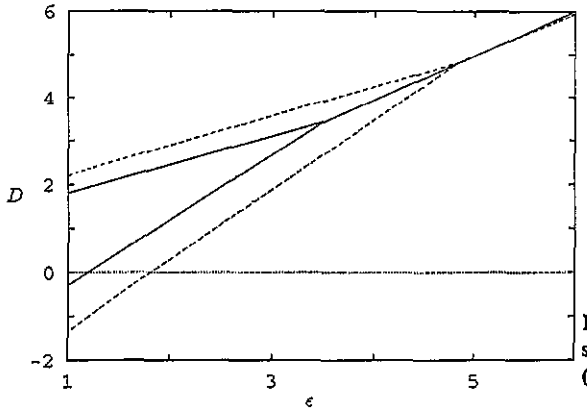

Figure 2. The phase diagram in the $(\epsilon - D)$ space for $T = 0$ (solid line) and $T = 2$ (dashed line).

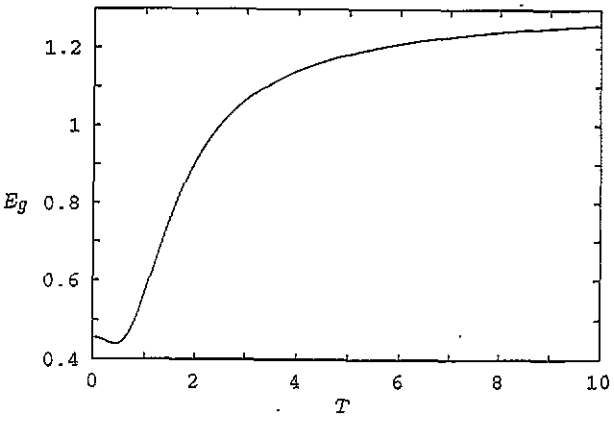

Figure 3. T-dependence of the energy gap in the Haldane phase for $\epsilon = 1$ and $D = 0$.

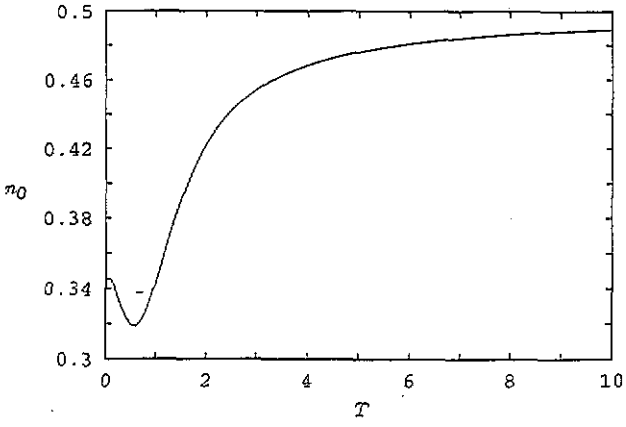

Figure 4. T-dependence of the defect concentration n_0 in the Haldane phase; parameters as in figure 3.

An interesting criterion to distinguish the phases is the q-dependence of Θ_q shown in figure 5. In the Haldane phase we have $\Delta\Theta = \Theta_\pi - \Theta_0 = \pi$, and in the other two phases, $\Delta\Theta = 0$.

Since our approach describes the quantum chain in terms of defects, it is interesting to investigate n_0 as a function of ϵ and D; the result is shown in figure 6. The Néel phase and the large-D phase correspond to the plateaus at, respectively,

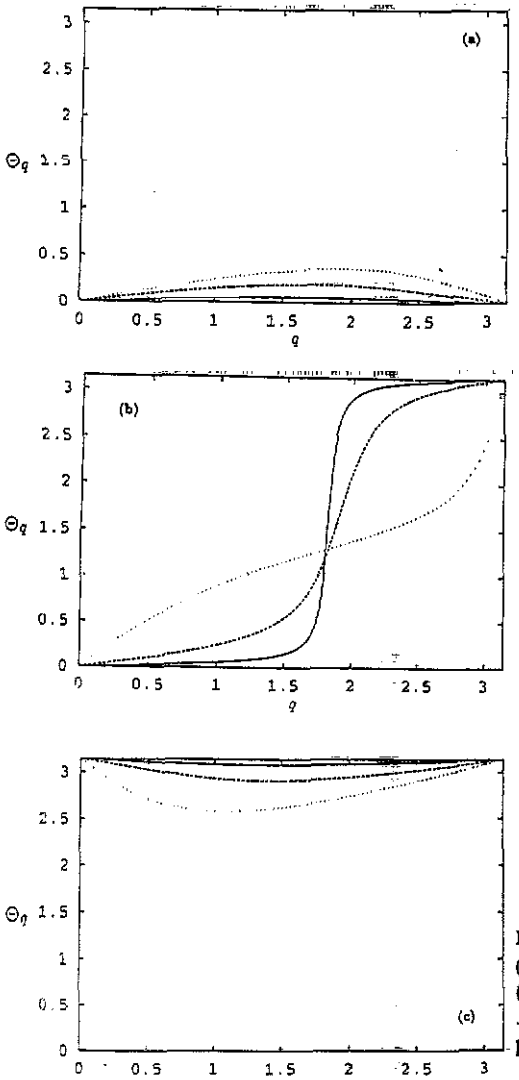

Figure 5. q-dependence of the angle Θ_q for $T = 0$ (dotted line), $T = 2$ (dashed line) and $T = 10$ (solid line) for $\epsilon = 1$; (*a*) $D = -4$ Néel phase, (*b*) $D = -0$ Haldane phase and (*c*) $D = 4$ large-D phase.

$n_0 \approx 0$ and $n_0 \approx 1$. The Haldane phase relates to the inclined part of the surface, where n_0 rises continuously from $n \approx 0$ to $n_0 \approx 1$. For larger values of ϵ and D (above the triple point at $\epsilon_t \approx 3.5$, $D_t \approx 3.5$), this increase becomes more abrupt.

The behaviour of n_0 is completed by the $(\epsilon - D)$-dependence of n_1, which is a measure of defect mobility. From the result (figure 7), it becomes obvious that the *Haldane phase* exhibits *maximum mobility*, in contrast to the Néel and large-D phases, in which n_1 is rather small.

3.3. Spin correlations

We have calculated the nearest and next-nearest neighbour spin correlation functions $\langle S_k^\alpha S_l^\alpha \rangle$ for $\alpha = z(|k-l| = 1,2)$ and for $\alpha = x(|k-l| = 1)$. For instance, the z–z-correlations can be expressed via the defect concentration operators as

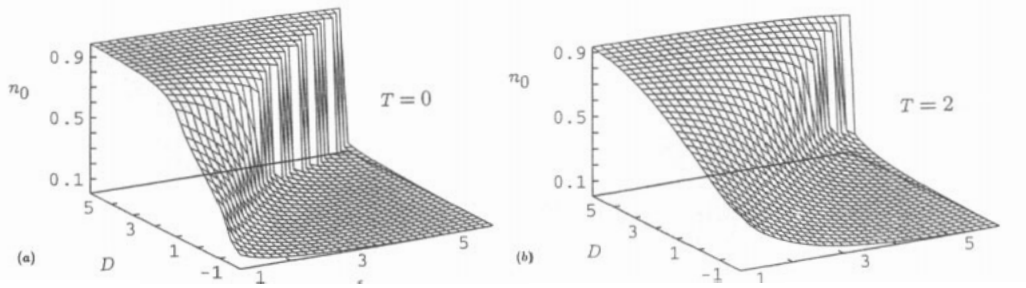

Figure 6. ϵ- and D-dependence of the defect concentration n_0 for (*a*) $T = 0$ and (*b*) $T = 2$.

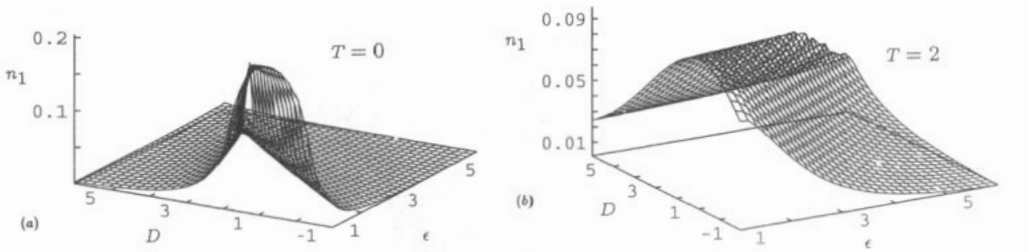

Figure 7. ϵ- and D-dependence of the 'mobility' n_1 for (*a*) $T = 0$ and (*b*) $T = 2$.

$$\langle S_k^z S_l^z \rangle = (-1)^{|k-l|} \left\langle (n_k - 1) \exp\left(i\pi \sum_{k<j<l} n_j \right) (n_l - 1) \right\rangle \tag{22}$$

The factors $(n_k - 1)$ and $(n_l - 1)$ take into account that $S_k^z S_l^z$ vanishes, provided a defect sits at site k or l. The exponential considers the number of defects between sites k and l, taking into account the sign of the correlation function. A similar representation is found for the x–x-correlations. Both types of correlations were determined within the mean field type of approximation we discussed in section 2 [cf (10)]. The results (depicted in figures 8 and 9) are consistent with those of n_0 and n_1 (presented in figures 6 and 7). For example, the nearest neighbour z–z-correlation (figure 8) is about -1 (corresponding to $n_0 = 0$) and 0 (corresponding to $n_0 = 1$) in the Néel and large-D phases, respectively, whereas the Haldane phase corresponds to the inclined part of the surface. The next-nearest neighbour z–z correlation (figure 8(*b*) remains small in the large-D phase and converges to $+1$ in the Néel phase, elucidating the antiferromagnetic order in the latter phase. The x–x-correlation was calculated for nearest neighbours only. The result (figure 9) compares favorably with figure 7, since $S_i^x\ S_j^x$ also induces defect motion.

3.4. Specific heat

Using the Hartree–Fock approximation, it is straightforward to determine the internal energy, from which we obtain the specific heat $C(T)$ (for zero external field). The result is shown for different ϵ and $D = 0$ (figure 10). A well-pronounced maximum (Schottky anomaly) exists, due to the existence of an energy gap at $T = 0$ K;

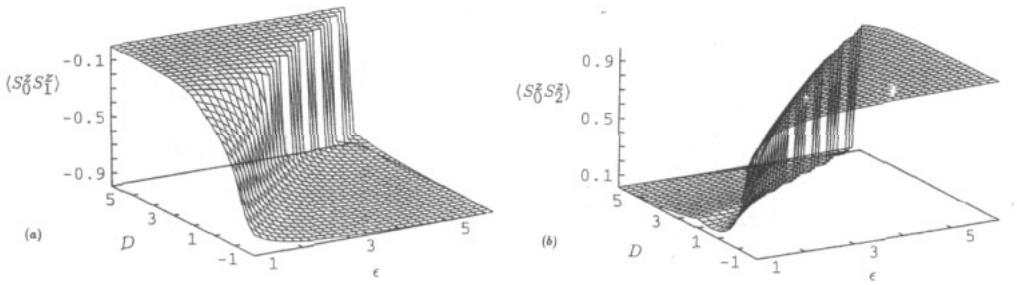

Figure 8. ϵ- and D- dependence of $\langle S_{i+n}^z S_i^z \rangle$ for $T = 0$: (*a*) $n = 1$, (*b*) $n = 2$.

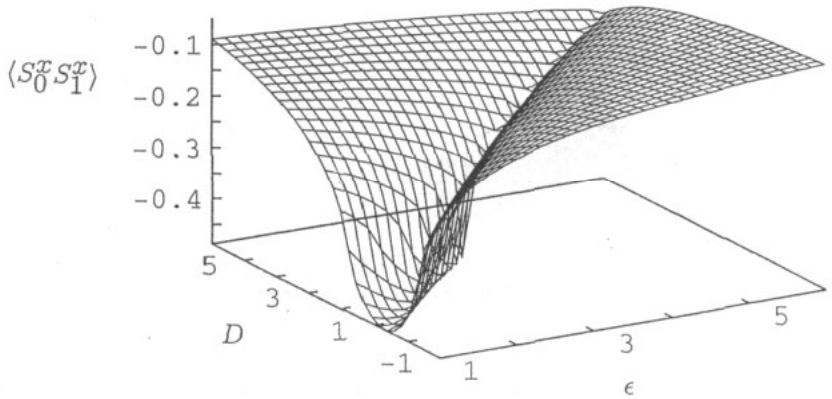

Figure 9. ϵ- and D-dependence of the nearest-neighbour spin correlation $\langle S_{i+1}^z S_i^z \rangle$ for $T = 0$.

its position is approximately proportional to ϵ for $\epsilon \geqslant 2$. For $T \to 0$, $C(T)$ vanishes *exponentially* if $E_g(T = 0) > 0$. The qualitative change for $C(T)$ when the gap energy $E_g(T = 0)$ decreases to zero is demonstrated in figure 11. At $E_g(T = 0) \to 0$ there is a crossover from exponential to power law decay. In case of $E_g(T = 0) = 0$, we find from figure 11 that $C(T)$ increases *linearly* with T. But it is also interesting that a linear behaviour exists over a finite T interval for finite gap energy $E_g(T = 0) > 0$.

4. Discussion and conclusions

In this paper we have extended the defect pattern, as recently suggested by Gómez-Santos [8], to a $s = 1$ Heisenberg antiferromaget, including single-ion anisotropy, and to finite temperatures. Two main approximations are involved in this approach. First, the Hilbert space is restricted to spin configurations mainly containing zero-spin defects; the ferromagnetic nearest-neighbour correlations are only taken into account by a variational method; the zero-spin defects are described as fermions. Second, the corresponding effective fermion Hamiltonian is treated in a Hartree–Fock approximation.

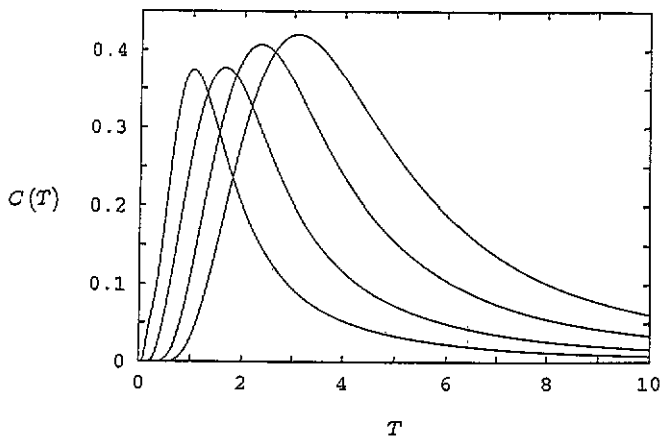

Figure 10. Specific heat $C(T)$ for $D = 0$ and $\epsilon = 1, 2, 3$ and 4.

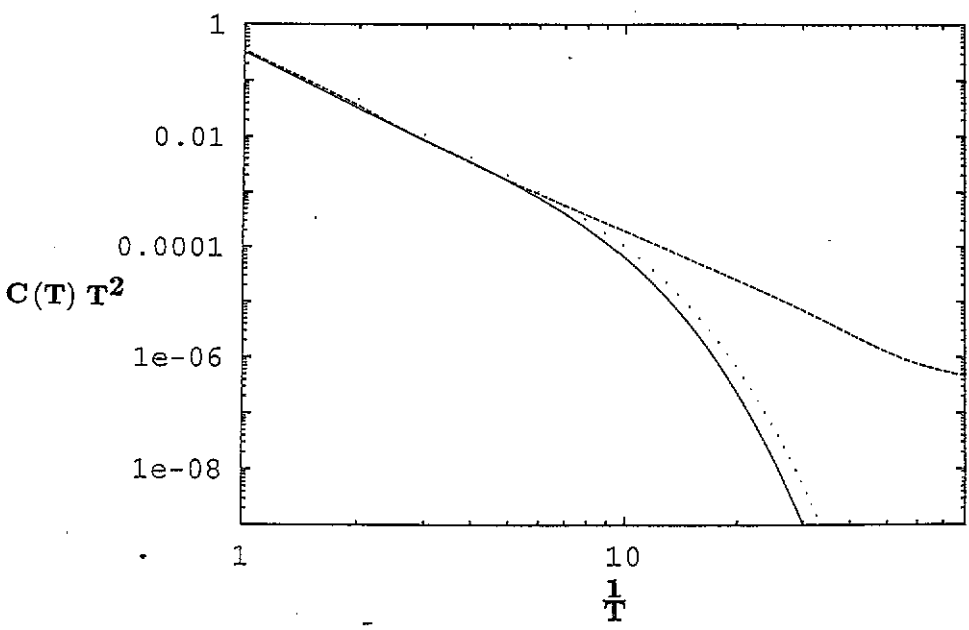

Figure 11. Double-logarithmic plot of $C(T)$ as a function of T for $D = 0$ and $\epsilon = 1$ (dotted curve), $\epsilon_c \approx 1.184$ (dashed curve) and $\epsilon = 1.4$ (solid curve).

The $\epsilon - D$ phase diagram is in good qualitative agreement with earlier results [4]–[8] for $\epsilon \geqslant 1$. We found three different phases in particular, which can be identified as the Néel, Haldane, and large-D phase. With the gap energy E_g as an order parameter, we found a second-order phase transition between all these phases. This does not imply that a first order transition may occur between the Néel and large-D phase if another order parameter is chosen (the string order parameter, e.g., exhibits a first-order phase transition [6]. Neglecting the x–y part of the Hamiltonian (1), it is easy to prove that the phase boundary between the Néel and large-D phases is

given by $\epsilon = D$, which is consistent with our result for $\epsilon \to \infty$ and $D \to \infty$. We were also able to show that the gap energy $E_g \sim \epsilon$ changes continuously, crossing the boundary $\epsilon = D$.

The defect approach also allows identification of the three phases by the defect concentration n_0 and defect mobility n_1. The Néel and large-D phases are well characterized by the asymptotic value $n_0 = 0$ (as $\epsilon \to \infty$) and $n_0 = 1$ (as $D \to \infty$), respectively. A smooth variation between $n_0 = 0$ and $n_0 = 1$ is typical for the Haldane phase (figure 6), a behaviour which is supported by the $(\epsilon - D)$-dependence of the defect mobility (figure 7). Since $n_0 \approx 0$ and $n_0 \approx 1$, the defect mobility is rather small in the Néel and large-D phases — its maximum value comes within the Haldane phase. These observations are consistent with the behaviour of the spin correlation functions and can be interpreted within a BCS-type description which, as far as we know, has not previously been noticed.

In fact, the ground state of the Hartree–Fock Hamiltonian ((12)) for the *spinless* fermions is given by the BCS-type state:

$$|\Psi_0\rangle = \prod_q \left(u_q + v_q c_q^\dagger c_{-q}^\dagger\right)|0\rangle \tag{23}$$

with u_q and v_q from ((15)). Note that $|0\rangle$ is the true vacuum state, not the occupied Fermi sphere. The low-level excitations

$$d_{q_0}^\dagger|\Psi_0\rangle = c_{q_0}^\dagger \prod_{q \neq q_0} \left(u_q + v_q c_q^\dagger c_{-q}^\dagger\right)|0\rangle \tag{24}$$

are related to the break-up of a 'Cooper pair' $c_{q_0}^\dagger c_{-q_0}^\dagger|0\rangle$. The corresponding gap energy between the Haldane phase and the two other phases vanishes.

Within the BCS-type description, the three phases can be characterized as follows. Taking into account that $\Theta_q \approx 0$ and $\Theta_q \approx \pi$ (cf figure 5(*a*) and (*c*)), it follows from ((16)) that $|u_q| \approx 1$, $v_q \approx 0$ and $u_q \approx 0$, $|v_q| \approx 1$, respectively. Thus, at $T = 0K$ the Néel phase ($\epsilon \to \infty$) does not contain 'Cooper pairs', whereas the large-D phase is a tensor product of $N/2$ pair states. In contrast, the *Haldane phase*, for which Θ_q changes from 0 to π (cf figure 5(*b*)), is characterized by $u_q \neq 0$ *and* $v_q \neq 0$ ($q \neq 0, \pi$), i.e. it is a BCS-phase of spinless fermions. This interpretation is also supported by the $(\epsilon - D)$-dependence of $h_1 = \frac{1}{N}\sum_q \langle c_q^\dagger c_{-q}^\dagger\rangle$ shown in figure 12.

Finally, we comment on the temperature dependence of these results. The phase diagram does not depend qualitatively on the temperature. Its topology remains unchanged (cf figure 2).

The T-dependent 'renormalized' gap energy $E_g(T)$ exhibits a minimum at a temperature T_{min} for the Haldane phase (figure 3(*b*)). For the other two phases, E_g is a monotonous function of T.

The specific heat $C(T)$ obtained exhibited a Schottky anomaly (figure 10). The position of the isotropic point was $T_{max} \approx 1.02$, which is about 10% above the result reported by de Neef *etal*, Campana *et al* [11] and Blöte [11], but about a factor four too large compared to Weng *et al* [11]. The value $C_{max} = C(T_{max})$ deviates more strongly, e.g. our value of $C_{max} \approx 0.37$ is about 40% too small when compared with Blöte's result [11], and even smaller than those of Weng *et al* and de Neef *et al* [11]. The reason for this discrepancy of C_{max} values is probably explained by our restriction of the Hilbert space which leads to underestimation of C_{max}.

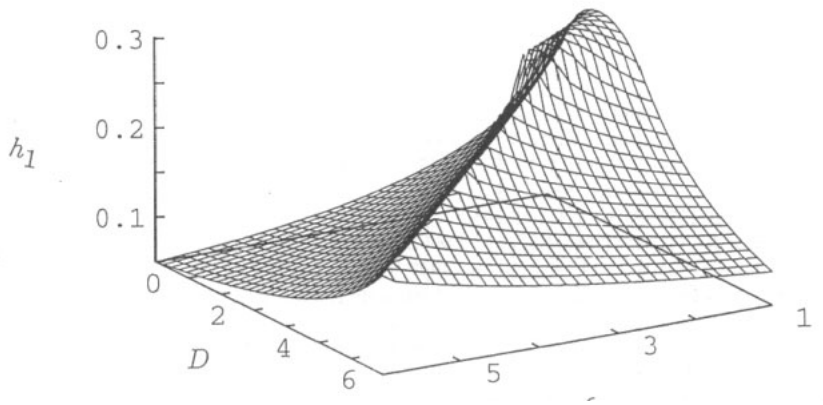

Figure 12. ϵ- and D-dependence of h_1 for $T = 0$.

Choosing ϵ and D at zero-temperature phase boundary ($T = 0$) between the Haldane phase and both other phases, $C(T)$ exibits a linear dependence up to $T = 0K$. *Within* the Haldane phase, a *finite* regime above $T = 0K$ but below T_{max} remains with a linear T-dependence (cf figure 11), which is in agreement with the results of Moses *et al* [11]. The double logarithmic plot for $C(T)$ (figure 11) also reveals a bend at a temperature $T \approx 0.5$, where the defect concentration and the gap energy develop an extremum. It is not obvious whether this particular type of T-dependence of $E_g(T)$ and $C(T)$ for the Haldane phase is genuine or a result of our approximations–it would be important to clarify this point by further experimental and theoretical investigations.

To summarize, we have demonstrated that the defect method for the Hamiltonian (1) leads to a qualitatively correct phase diagram, the topology of which does not change with temperature. It was shown that the Haldane phase can be interpreted as a BCS–state of spinless fermions and the excitations as a break-up of 'Cooper pairs'. The specific heat is in good agreement with earlier results. It exhibits a linear part and a bend for $T < T_{max}$. This bending point is in correspondence with a minimum in $E_g(T)$.

Note added in proof. After submission of this manuscript, a paper by Mikeska [15] has appeared with a similar analysis of the defect approach but only for $T = 0$.

References

[1] Haldane F D M 1983 *Phys. Lett.* **93A** 464; 1983 *Phys. Rev. Lett.* **50** 1153

[2] Affleck I, Kennedy T, Lieb E H and Tasaki H 1987 *Phys. Rev. Lett.* **59** 799; 1988 *Commun. Math. Phys.* **115** 477

[3] Steiner M, Kakurai K, Kjems J K, Petitgrand D and Pynn R 1987 *J. Appl. Phys.* **61** 3953
Buyers W J L, Morra R M, Armstrong R L, Horgan M J, Gerlach P and Hirakawa K 1986 *Phys. Rev. Lett.* **56** 371
Tun Z, Buyers W J L, Armstrong R L, Hallman E D and Arovas D P 1989 *Proc. Int. Conf. Magnetism (Paris) 1988 J. Physique Coll.* **49** C8 1431
Renard J P, Verdaguer M, Regnault L P, Erkelens W A C, Rossat-Mignod J and Stirling W G 1987 *Europhys. Lett.* **3** 945

[4] Botet R, Jullien R and Kolb M 1983 *Phys. Rev.* B **28** 3914
[5] Solyom J and Ziman T 1984 *J. Appl. Phys.* **57** 3319
Glaus U and Schneider T 1984 *Phys. Rev.* B **30** 215
Parkinson J B, Bonner J C, Müller G, Nightingale M P and Blöte H W J 1985 *J. Appl. Phys.* **57** 3319
Parkinson J B and Bonner J C 1985 *Phys. Rev.* B **32** 4703
Nightingale M P and Blöte H W J 1986 *Phys. Rev.* **33** 659
Schulz H J and Zimon T 1986 *Phys. Rev.* B **33** 6545
Schulz J J 1986 *Phys. Rev.* B **34** 6372
Glaus U 1987 *Physica* A **141** 295
Saitoh K, Takada S and Kubo K 1987 *J. Phys. Soc. Japan* **56** 3755
Bonner J C 1987 *J. Appl. Phys.* **61** 3941
[6] den Nijs M and Rommelse K 1989 *Phys. Rev.* B **40** 4709
Girvin S M and Arovas D P 1989 *Phys. Scr.* T **27** 156
Hatsugai Y and Kohmoto M 1991 *Phys. Rev.* B **44** 11789
[7] Tasaki H 1990 *Phys. Rev. Lett* **64** 2066; 1991 *Phys. Rev. Lett* **66** 798
[8] Gómez-Santos G 1989 *Phys. Rev. Lett.* **63** 790
[9] The defect-picture has also been applied to $s = \frac{1}{2}$ (Gómez-Santos G 1990 *Phys. Rev.* B **41** 6788). In accordance with Haldane's conjecture, no gap was found.
[10] Delica T, Kopinga K, Leschke H and Mon K K 1991 *Europhys. Lett.* **15** 55
[11] Weng C Y and Griffiths R B 1968 unpublished
de Neef T and de Jonge W J M 1975 *Phys. Rev.* B **11** 4402
Blöte H W J 1975 *Physica* B **79** 427
Campana L S, Caramico A, Auria D, Esposito F, Esposito U and Kamieniarz G 1992 *Phys. Rev.* B **45** 5035
[12] Moses D, Schechter H, Ehrenfreund E and Maeovsky J 1977 *J. Phys. C: Solid State Phys.* **10** 433
Iio K, Hyodo H and Nagota K 1980 *J. Phys. Soc. Japan* **49** 1336
[13] van Hemmen J L 1980 *Z. Phys.* **38** 271
[14] Nightingale M P and Blöte H J W 1986 *Phys. Rev.* B **33** 659
[15] Mikeska H J 1992 *Europhys. Lett.* **19** 34–44
[16] Kakurai K, Steiner M, Pynn P and Kjems J K 1991 *J. Phys.: Condens. Matter* **3** 715–726